

Exploring the level sets of quantum control landscapes

Adam Rothman,^{*} Tak-San Ho,[†] and Herschel Rabitz[‡]

Department of Chemistry, Princeton University, Princeton, New Jersey 08544-1009, USA

(Received 8 July 2005; published 1 May 2006)

A quantum control landscape is defined by the value of a physical observable as a functional of the time-dependent control field $E(t)$ for a given quantum-mechanical system. Level sets through this landscape are prescribed by a particular value of the target observable at the final dynamical time T , regardless of the intervening dynamics. We present a technique for exploring a landscape level set, where a scalar variable s is introduced to characterize trajectories along these level sets. The control fields $E(s,t)$ accomplishing this exploration (i.e., that produce the same value of the target observable for a given system) are determined by solving a differential equation over s in conjunction with the time-dependent Schrödinger equation. There is full freedom to traverse a level set, and a particular trajectory is realized by making an *a priori* choice for a continuous function $f(s,t)$ that appears in the differential equation for the control field. The continuous function $f(s,t)$ can assume an arbitrary form, and thus a level set generally contains a family of controls, where each control takes the quantum system to the same final target value, but produces a distinct control mechanism. In addition, although the observable value remains invariant over the level set, other dynamical properties (e.g., the degree of robustness to control noise) are not specifically preserved and can vary greatly. Examples are presented to illustrate the continuous nature of level-set controls and their associated induced dynamical features, including continuously morphing mechanisms for population control in model quantum systems.

DOI: [10.1103/PhysRevA.73.053401](https://doi.org/10.1103/PhysRevA.73.053401)

PACS number(s): 32.80.Qk, 11.27.+d

I. INTRODUCTION

The control of quantum phenomena is an increasingly active area of research [1,2]. Quantum control theory [3–11] has provided many of the concepts [12] behind the performance of recent closed-loop control experiments [13–19]. The search for an effective control is often carried out as an optimization on a landscape, which is defined as the target observable value as a functional of the control field for a given (constant) quantum system. Some basic features of the control landscapes are beginning to emerge [20], but much remains to be understood. This paper provides one means for exploring quantum control landscapes by taking trajectories over their level sets, specified by a particular value of the observable.

The quantum control landscape for a given Hamiltonian is generally expected to be a highly complicated functional of the control field. A point on the landscape corresponds to the observable value derived from a particular control field at a constant final dynamical time T . Consideration of all possible control fields would specify the full landscape, while a level set would consist of the collection of all fields that produce a particular value for the target observable, regardless of the intervening temporal dynamics (i.e., control mechanism).

Exploration of level sets through the control landscape is important for several fundamental reasons. The existence of multiple control field solutions to a given quantum control problem has been known for some time [21–23]; however, if

these distinct solutions are interpreted as members of the same quantum control landscape level set, the relationship between them may be better understood, particularly if a trajectory through the landscape may be identified that links the solutions. In addition, a level-set analysis may be the first step to understanding the complete relationship between tailored fields and controlled quantum dynamics as level-set explorations can systematically explore the quantum control landscape in order to learn more about the topology of the space.

This paper presents a simple trajectory technique for traversing the level sets in arbitrary directions. In doing so, the physical system need not be fully controllable, but the level-set observable value must be reachable. The tools utilized for the control level-set analysis are a special case of a broader technique referred to as diffeomorphic modulation under observable preserving homotopy (D-MORPH) [24]. The remainder of the paper is organized as follows. Section II derives the formalism for exploring level sets in the control landscape, and numerical examples are presented in Sec. III. Finally, concluding remarks are provided in Sec. IV.

II. LEVEL-SET CONTROL ANALYSIS

This section develops a simple means for exploring level sets on a quantum control landscape. At the final dynamical time T , the expectation value of the target observable operator \mathcal{O} of interest is given by $\langle\psi(T)|\mathcal{O}|\psi(T)\rangle\equiv\langle\mathcal{O}\rangle$, where $|\psi(t)\rangle$ satisfies the time-dependent Schrödinger equation on the interval $t\in[0,T]$,

^{*}Electronic address: arothman@princeton.edu

[†]Electronic address: tsho@princeton.edu

[‡]Electronic address: hrabitz@princeton.edu

$$i\hbar \frac{\partial}{\partial t} |\psi(t)\rangle = [\mathcal{H}_0 - \mu E(t)] |\psi(t)\rangle, \quad |\psi(0)\rangle = |\psi_0\rangle, \quad (1)$$

for the field-free Hamiltonian \mathcal{H}_0 and dipole matrix operator μ , with $E(t)$ being the control field and $|\psi_0\rangle$ the initial condition. The level-set analysis depends on the mapping $E(t) \rightarrow \langle \mathcal{O} \rangle$, and other forms of the Hamiltonian can just as easily be treated. A variation of $\langle \mathcal{O} \rangle$ due to an associated differential variation $\delta E(t)$ is given to first order by

$$d\langle \mathcal{O} \rangle = \int_0^T \frac{\delta \langle \mathcal{O} \rangle}{\delta E(t)} dE(t) dt. \quad (2)$$

The higher-order terms neglected in Eq. (2) only become relevant at a true control extremum, where $\frac{\delta \langle \mathcal{O} \rangle}{\delta E(t)} = 0, \forall t$. In this paper, exploration of the landscape level sets will be done away from an extremum, but an extremum may be approached numerically as close as desired with the present formulation. Since the goal of the analysis is to explore level sets of the quantum control landscape, it is convenient to parametrize the field and its variation by the exploration variable s ,

$$E(t) \Rightarrow E(s, t), \quad (3a)$$

$$dE(t) \Rightarrow dE(s, t). \quad (3b)$$

Here, s spans some domain and without loss of generality we may take $0 \leq s \leq 1$, where the initial control field $E(s=0, t)$ is assumed known from some prior control calculation. Dividing Eq. (2) by the differential ds produces

$$\frac{d}{ds} \langle \mathcal{O} \rangle = \int_0^T \frac{\delta \langle \mathcal{O} \rangle}{\delta E(s, t)} \frac{\partial E(s, t)}{\partial s} dt = 0, \quad (4)$$

where the right-hand side has been set to zero in recognition of the fact that level sets on the quantum control landscape are defined by the demand $\frac{d}{ds} \langle \mathcal{O} \rangle = 0, \forall s$, corresponding to the observable value remaining invariant [i.e., fixed at the value determined by $E(0, t)$] while the control field $E(s, t)$ traverses some trajectory parametrized by s . The possible dependence of $\langle \mathcal{O} \rangle$ on s is evident in the expression $\langle \mathcal{O}(s) \rangle = \langle \psi(s, T) | \mathcal{O} | \psi(s, T) \rangle$, where $|\psi(s, T)\rangle$ depends on s through $E(s, t)$; traversing a level set corresponds to identifying control field trajectories $E(s, t)$, $s > 0$, such that $\langle \mathcal{O}(s) \rangle = \langle \mathcal{O}(s=0) \rangle$, $s > 0$. The relationship in Eq. (4) is highly underspecified for determining $E(s, t)$ as s traverses a level set, and the integral equation may be conveniently expressed as an equivalent initial-value problem

$$\frac{\partial E(s, t)}{\partial s} = S(t) \left\{ f(s, t) - \frac{\gamma(s)}{\Gamma(s)} a_0(s, t) \right\}, \quad (5)$$

where $E(0, t)$ is assumed to be known. Here, $S(t)$ is an arbitrary weight function (used, for example, to bias the control field towards a short pulse that approaches zero at $t=0$ and $t=T$) and the notational choice $a_0(s, t) \equiv \frac{\delta \langle \mathcal{O} \rangle}{\delta E(s, t)}$ is made in keeping with earlier D-MORPH work [24]. The function $a_0(s, t)$ may be identified as (see the Appendix)

$$a_0(s, t) = -\frac{1}{i\hbar} \langle \psi_0 | [U^\dagger(T, 0) \mathcal{O} U(T, 0), U^\dagger(t, 0) \mu U(t, 0)] | \psi_0 \rangle, \quad (6)$$

where $U(t, t')$ is the time evolution operator satisfying

$$i\hbar \frac{\partial}{\partial t} U(t, 0) = [\mathcal{H}_0 - \mu E(s, t)] U(t, 0), \quad U(0, 0) = \mathbf{I}. \quad (7)$$

Since $U(t, 0)$ depends on the control field $E(s, t)$, it is understood to depend on s as well.

For convenience below, we introduce the weighted inner-product notation

$$(p(s), q(s))_{S(t)} = \int_0^T S(t) p(s, t) q(s, t) dt, \quad (8)$$

where $p(s, t)$ and $q(s, t)$ are arbitrary integrable functions of $t \in [0, T]$. In this notation, the initial-value problem, Eq. (5), employs

$$\Gamma(s) = (a_0(s), a_0(s))_{S(t)} \quad (9a)$$

and

$$\gamma(s) = (a_0(s), f(s))_{S(t)}. \quad (9b)$$

The validity of Eq. (5) for any continuous function $f(s, t)$ of arbitrary form [25] can easily be verified by substitution into Eq. (4). The origin of the ability to *freely choose* the functions $f(s, t)$ lies in the multiplicity of solutions to the original equation (4). Thus, by construction, regardless of the choice made for the function $f(s, t)$ in Eq. (5), the observable $\langle \mathcal{O}(s) \rangle$ will remain invariant. A particular choice for $f(s, t)$ will result in the field $E(s, t)$ traversing a particular trajectory, labeled by s , across the level set.

The working equations to traverse the level sets are Eqs. (5) and (7), which are linked through $a_0(s, t)$ in Eq. (6). Additional insight into how $f(s, t)$ in Eq. (5) guides the level set trajectories may be obtained by defining $u_{\mathcal{O}}(s, t)$ as a function of unit norm under the weighted inner product, Eq. (8),

$$u_{\mathcal{O}}(s, t) = a_0(s, t) / \Gamma(s)^{1/2}, \quad (10)$$

such that

$$(u_{\mathcal{O}}(s), u_{\mathcal{O}}(s))_{S(t)} = 1. \quad (11)$$

A projection operator $\mathcal{P}_{\mathcal{O}}$ can be specified in terms of the function $u_{\mathcal{O}}(s, t)$, where the action of $\mathcal{P}_{\mathcal{O}}$ on any continuous function $f(s, t)$ is

$$\mathcal{P}_{\mathcal{O}} \cdot f(s, t) = u_{\mathcal{O}}(s, t) (u_{\mathcal{O}}(s), f(s))_{S(t)}. \quad (12)$$

Equation (5) may then be rewritten as

$$\frac{\partial E(s, t)}{\partial s} = S(t) [1 - \mathcal{P}_{\mathcal{O}}] f(s, t) = S(t) g(s, t). \quad (13)$$

By virtue of the identity $a_0(s, t) = \frac{\delta \langle \mathcal{O} \rangle}{\delta E(s, t)}$ in Eq. (6), the operator $1 - \mathcal{P}_{\mathcal{O}}$ projects any choice of $f(s, t)$ to produce a function $g(s, t)$ that has no component along the direction [i.e., $a_0(s, t)$

or, equivalently, $u_{\mathcal{O}}(s,t)$ that could change $\langle \mathcal{O}(s) \rangle$, since Eqs. (4) and (13) imply that

$$\int_0^T a_0(s,t) \frac{\partial E(s,t)}{\partial s} dt = (a_0(s,t), g(s,t))_{S(t)} = 0. \quad (14)$$

In this fashion, formally integrating Eq. (13) yields a control $E(s,t)$,

$$E(s,t) = E(0,t) + S(t) \int_0^s g(s',t) ds', \quad (15)$$

which produces dynamics that leaves $\langle \mathcal{O}(s) \rangle$ invariant [i.e., $\langle \mathcal{O}(s) \rangle = \langle \mathcal{O}(s=0) \rangle$] at the final dynamical time T . However, the intervening dynamics over the interval $t \in [0, T]$ for any particular value of s will generally be very sensitive to the path that $E(s,t)$, $s > 0$, follows along the level set. Thus, although the target observable $\langle \mathcal{O}(s) \rangle$ remains fixed regardless of the value of s over a trajectory along the landscape level set, the control mechanism is not conserved and could vary widely over the span of the level set. Furthermore, other dynamical characteristics could also vary over the level set; an important characteristic is robustness to control field noise reflected in the observable's Hessian eigenvalues. These points will be made evident in the illustrations of the following sections.

To facilitate understanding the notion of a trajectory through a level set of the quantum control landscape, a metric $D_s[E]$ is defined that measures the distance between any control field $E(s,t)$ on a level-set path and the corresponding initial control field $E(0,t)$ as follows:

$$\begin{aligned} D_s[E] &\equiv \|E(s,t) - E(0,t)\|_2 \\ &= \left(\frac{1}{T} \int_0^T [E(s,t) - E(0,t)]^2 dt \right)^{1/2} \\ &= \left[\frac{1}{T} \int_0^T \left(S(t) \int_0^s g(s',t) ds' \right)^2 dt \right]^{1/2}, \quad (16) \end{aligned}$$

where the last step utilized Eq. (15). The metric $D_s[E]$ is positive semi-definite (i.e., $D_s[E] \geq 0$ and $D_s[E] = 0 \Leftrightarrow E(s,t) = E(0,t)$) and easy to compute. As $g(s,t)$ is a free function with the only criterion being that it be orthogonal to $u_{\mathcal{O}}(s,t)$ [cf. Eq. (14)], it is evident that some level-set excursions can lead $D_s[E]$ to grow without bound. In this metric sense, the level sets are generally expected to be of infinite extent while always preserving $\langle \mathcal{O}(s) \rangle$, yet exhibiting a continuous family of control mechanisms.

III. NUMERICAL EXAMPLES

The illustrations in this section aim to demonstrate the freedom imparted by the continuous function $f(s,t)$ for the evolution of the control fields $E(s,t)$ and their associated mechanisms across quantum control level sets. However, since the focus of this paper is to introduce the level-set technique, the physical systems considered here are deliber-

ately simple and no attempt is made to draw a comparison between the systems considered in this section and systems used in laboratory control experiments, although the principle applies equally well to both circumstances. All of the calculations consider an eight-level Hamiltonian of the form described in Eq. (1) [26] with nondegenerate levels and where the only allowed couplings are between adjacent, next-nearest, and next-next-nearest states. The control goal in the examples is state-to-state population transfer from $|1\rangle$ to $|8\rangle$ over the interval $t \in [0, T]$ at a particular yield specifying the level set through which trajectories will be taken. The intermediate-time dynamics (i.e., control mechanism) is not constrained and varies freely along the level-set trajectory. For these illustrations, $\mathcal{O} = |f\rangle\langle f|$ with $|f\rangle = |8\rangle$, so that Eq. (6) reduces to

$$a_0(s,t) = -\frac{2}{\hbar} \text{Im}\{\langle \psi_0 | U^\dagger(T,0) | f \rangle \langle f | U(T,t) \mu U(t,0) | \psi_0 \rangle\}. \quad (17)$$

The goal is to show that for a given input control field $E(s=0,t)$, various choices of $f(s,t)$ lead to different trajectories along the landscape level-set traversing fields that preserve the value of the target observable but exhibit different characteristics, both in the pulse shape and in the induced quantum dynamics. These characteristics will provide evidence of the breadth of the field and dynamical behavior found in any particular level set. Furthermore, the opportunity exists for specifying a level-set pathway along which specific control field characteristics are imposed through the choice of $f(s,t)$, although this capability is not directly addressed here. The metric $D_s[E]$ will be used as a quantitative measure of the breadth of the level set, as viewed from the reference field $E(0,t)$.

Computationally, Eq. (5) is solved using fourth-order Runge-Kutta integration over s , where each derivative evaluation requires solving the time-dependent Schrödinger equation (1) subject to the control field at the most recent s step. Within each evaluation of $\frac{\partial E(s,t)}{\partial s}$ [i.e., the right-hand side of Eq. (5)], the time variable t is uniformly discretized as t_j , $j=0, 1, \dots, n-1$, where n is typically 1024 or 2048 and the extrema of the interval are $t_0=0$ and $t_{n-1}=T=14$. To obtain the coefficient $a_0(s,t)$, the Schrödinger equation is propagated from $|\psi_0\rangle$ over the dynamical interval $t \in [0, T]$ by explicitly generating the time evolution matrices U_j , where each matrix $U_j = U(t_j, t_{j+1})$ evolves the wave function over the j th time step. Arbitrary units are used throughout.

A. Level sets for high control field

This case aims to explore the scope of the level set originating from an input control field $E(s=0,t)$ that produces the high yield $P_{|1\rangle \rightarrow |8\rangle} = 0.99$. To perform trajectories through the level set based on Eq. (5), we choose the functions

$$f(s,t) = f_{\pm}(s,t) = \pm \frac{E(s,t)}{c_{\pm}S(t)\Delta s}, \quad (18)$$

where Δs is the mesh spacing used in evolving the control fields, $S(t) = \exp\left(-\frac{(T-5.5)^2}{(T/5)^2}\right)$ is the weight function, and the constants $c_+ = 600$ and $c_- = 100$ are used to maintain numerical stability in solving for $E(s,t)$. It can be shown [24] that this choice of function will either maximize (+) or minimize (-) the fluence of the control field when moving towards large s values along the level set. Although fluence minimization is generally a desirable property in a control field, the consideration of fluence maximization in this section is a convenient way of moving as far away as possible (in terms of the field metric $D_s[E]$) from the initial field along a particular level set trajectory. In this regard, the \pm signs in Eq. (18) are critical to the analysis, while the presence of $c_{\pm}S(t)\Delta s$ simply scales the rate at which the excursion takes place. A larger constant c_+ is utilized for fluence maximization (over that of fluence minimization with c_-) because if the amplitude of the field grows too large, the temporal discretization needs to be finer in order to accurately propagate the Schrödinger equation.

The progression of fields $E_+(s,t)$ and $E_-(s,t)$ [i.e., corresponding to $f_{\pm}(s,t)$ in Eq. (18)] are displayed in Fig. 1(a), with each starting from the same initial field $E(s=0,t)$. It is evident that fluence maximization causes $E_+(s,t)$ to grow in amplitude and significantly change in form, while fluence minimization causes a decline in intensity in $E_-(s,t)$ that is far less dramatic in this case. Figure 1(b) makes the differences in control field evolution clearer by plotting $E(s=0,t)$ along with $E_+(s=1,t)$ and $E_-(s=1,t)$. Fluence minimization has an effect on the control field, although the effect is subtler than in the fluence maximizing case. There is some residual similarity in the fields as a result of $f_{\pm}(s,t)$ being proportional to $E(s,t)$ in Eq. (18). However, other choices for $f(s,t)$ can generate fields showing no such similarity yet still leaving $P_{|1\rangle \rightarrow |8\rangle} = 0.99$. To show the wide variety of dynamical behavior produced by these fields, Fig. 1(c) displays the population of state $|8\rangle$ as a function of t for the initial field $E(s=0,t)$ and at $s=1$ for the cases of fluence minimization and maximization. Importantly, the population in state $|8\rangle$ at the final dynamical time T is constant for all s , demonstrating that the progression of control fields $E(s,t)$ form a level set at $P_{|1\rangle \rightarrow |8\rangle} = 0.99$, independent of s . However, the intermediate-time dynamics depends on s and the imposed level-set trajectory in a very complicated way. The differences in the population of state $|8\rangle$ as a function of time are taken as evidence of the different control mechanisms operative in each case. In the present circumstance, the field at $s=1$ for fluence minimization is close to that of the initial field $E(s=0,t)$, which is reflected in their similar dynamics for the population in state $|8\rangle$ in Fig. 1(c). On the other hand, the case of fluence maximization shows significantly different population dynamics. These dynamical features indicate the use of multiple transition pathways throughout the s interval even in this illustration of just two level-set trajectories, suggesting that the level set specified by $P_{|1\rangle \rightarrow |8\rangle} = 0.99$

is vast and rich with fields capable of producing dynamics of dramatically different character.

To quantitatively assess the scope of the level set, Fig. 1(d) shows the metric $D_s[E_{\pm}]$ for $s \in [0, 1]$. As $s \rightarrow 1$, there is rapid growth in $D_s[E_+]$. Cutting off the level-set trajectory at $s=1$ is an arbitrary choice, and as indicated by Eq. (16) the growth of $D_s[E_+]$ can continue without bound along the level-set trajectory defined by $f_+(s,t)$ by proceeding to larger values of s . In contrast, the field metric $D_s[E_-]$ for the fluence minimizing case asymptotes as s increases, suggesting the arrival at a control field of minimal fluence that still accomplishes the required population transfer. This behavior may be further understood by considering the fluence minimizing cost functional J_- ,

$$J_-(s, [E_-(s,t)], [\langle \mathcal{O}(s) \rangle]) = \frac{1}{2} \int_0^T \frac{[E_-(s,t)]^2}{S(t)} dt - \frac{1}{\lambda} [\langle \mathcal{O}(s) \rangle - \langle \mathcal{O}(0) \rangle], \quad (19)$$

which is written within the more general context of an arbitrary observable $\langle \mathcal{O}(s) \rangle \equiv \langle \psi(s, T) | \mathcal{O} | \psi(s, T) \rangle$. Here, λ is a Lagrange multiplier introduced to satisfy the level-set constraint $\langle \mathcal{O}(s) \rangle = \langle \mathcal{O}(0) \rangle$, $\forall s$. The functional extremum of Eq. (19), $\frac{\delta J_-}{\delta E_-(s,t)} = 0$, in the asymptotic limit of $s \rightarrow \infty$ produces the relation

$$S(t) \frac{\delta \langle \mathcal{O} \rangle}{\delta E_-(t)} = \lambda E_-(t) \quad (20a)$$

or, equivalently,

$$S(t) a_0(t) = \lambda E_-(t), \quad (20b)$$

where $a_0(t)$ is given by Eq. (6). Here the dependence on s is suppressed, as Eq. (20) is assumed to be in the limit $s \rightarrow \infty$ with $a_0(t) = \lim_{s \rightarrow \infty} a_0(s, t)$ and $E_-(t) = \lim_{s \rightarrow \infty} E_-(s, t)$. Expressed another way, we expect that $\lim_{s \rightarrow \infty} \frac{\delta \langle \mathcal{O} \rangle}{\delta E_-(s,t)} = 0$, corresponding to producing a limiting field of minimal fluence as s grows, which is verified in Fig. 1(d) for $D_s[E_-]$. From Eqs. (5) and (18) in this case we have that

$$S(t) a_0(t) = \frac{\Gamma}{c_- \gamma \Delta s} E_-(t), \quad (21)$$

where the dependence on s disappears for $a_0(t)$, Γ , γ , and $E_-(t)$ in the limit $s \rightarrow \infty$. Equation (21) has the same form as Eq. (20b) with λ identified as $\Gamma/c_- \gamma \Delta s$. Importantly, Eq. (20b) can be viewed as a highly nonlinear integral equation eigenvalue problem with $a_0(t)$ given by Eq. (6) and the eigenfunctions and eigenvalues being $E_-^i(t)$ and λ^i , respectively. Here, the index i labels these eigenfunctions and eigenvalues; evidently, distinct fluence minimizing controls $E_0^i(t)$ may exist whose form depends on the initial choice for $E^i(s=0,t)$ such that $\lim_{s \rightarrow \infty} E^i(s,t) = E^i(t)$. Trajectories may be taken to discern the family of fluence minimizing fields $E_-^i(t)$ or Eq. (20b) could be solved iteratively for this purpose.

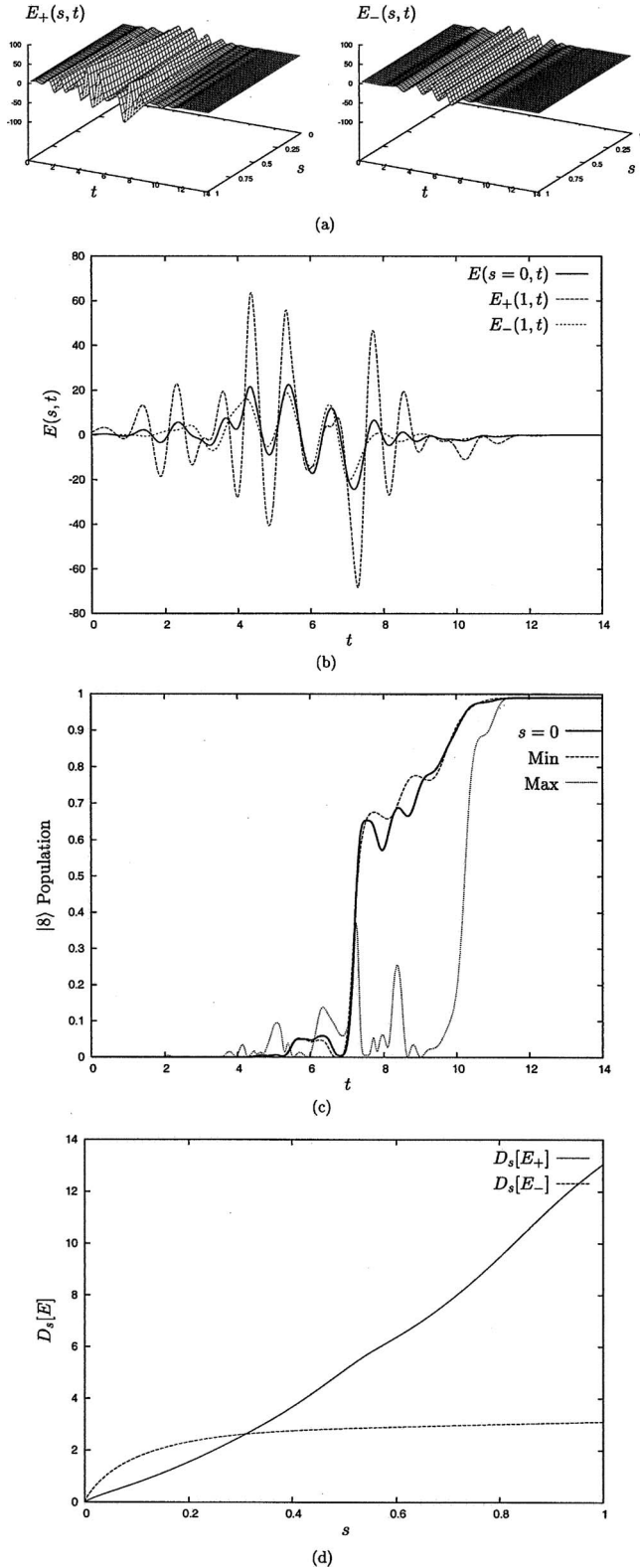


FIG. 1. Starting from an initial control field $E(s=0,t)$ and using 1024 s steps on the interval $s \in [0,1]$, the control fields $E_{\pm}(s,t)$ are evolved subject to the functions $f_{\pm}(s,t)$ in Eq. (18). (a) Under fluence maximization with $f_+(s,t)$, the control field grows in amplitude and incorporates complex structure; under fluence minimization with $f_-(s,t)$, the progression of fields decreases in amplitude, slightly in this case. (b) Cross sections of the fields in (a) at $s=0$ and $s=1$ are plotted. The field at $s=0$ is the same for $E_+(0,t)$ and $E_-(0,t)$, but the different functions $f_+(s,t)$ and $f_-(s,t)$ lead the fields to evolve in dramatically different ways for $s>0$. In particular, $E_+(1,t)$ incorporates new structure while $E_-(1,t)$ remains closer in structure to the original field. (c) The population of state $|8\rangle$ is displayed at $s=0$ and also at $s=1$ for both the fluence minimizing and maximizing cases. It is seen that fluence minimization tends to simplify the intermediate-time dynamics, while fluence maximization tends to complicate the dynamics. In all cases, the population at the final dynamical time $t=T$ is preserved. The differences in the intermediate-time dynamics here are taken as evidence of broader differences in the control mechanism along each level set trajectory. (d) The field metric $D_s[E]$, defined in Eq. (16), is plotted for fluence minimization and maximization. For fluence maximization, the metric increases rapidly with s ; under fluence minimization, the metric levels off as the field approaches minimal fluence while still accomplishing the requisite population transfer.

Level sets are defined by a constant value of the target observable, and the trajectories dictated by $f_{\pm}(s,t)$ obey this demand. However, while the target observable value is fixed, no such demand is made of other system observables and properties. One important quantity is the Hessian with respect to the control field,

$$\mathcal{H}(t,t') = \frac{\delta^2 P_{|1\rangle \rightarrow |8\rangle}}{\delta E(s,t) \delta E(s,t')} = \frac{\delta a_0(s,t')}{\delta E(s,t)}. \quad (22)$$

Employing the calculus of variations, Eq. (22) may be expressed as

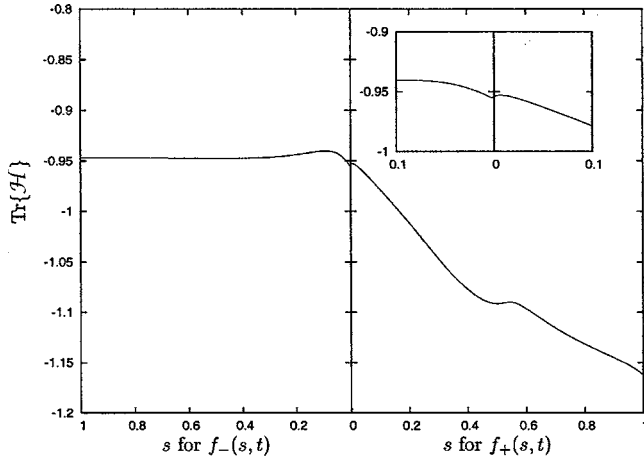


FIG. 2. The trace of the Hessian in Eq. (22) as a function of $s \in [0, 1]$ is shown for the high-yield level set example along both the fluence minimizing [$f_-(s, t)$] and fluence maximizing [$f_+(s, t)$] trajectories. Starting from the central axis ($s=0$), the s parameterization of the two trajectories points in opposite directions along the abscissa. Inset: close-up of the behavior near $s=0$. The cusp in the plot is due to a discontinuity in the derivative $\frac{\partial E(s, t)}{\partial s}$ caused by the different constants c_+ and c_- in $f_{\pm}(s, t)$ [cf. Eqs. (5) and (18)].

$$\begin{aligned} \mathcal{H}(t, t') = & \frac{2}{\hbar^2} \text{Re}\{\langle \psi_0 | \mu(t') U^\dagger(T, 0) | f \rangle \langle f | U(T, 0) \mu(t) | \psi_0 \rangle \\ & - \langle \psi_0 | U^\dagger(T, 0) | f \rangle \langle f | U(T, 0) \mu(t) \mu(t') | \psi_0 \rangle\}, \quad t \geq t', \end{aligned} \quad (23)$$

where the dipole operator matrix is, in the Heisenberg representation,

$$\mu(t) = U^\dagger(t, 0) \mu U(t, 0). \quad (24)$$

Equation (23) was evaluated at the discretized time points t_j , $j=0, 1, \dots, 2047$, and the Hessian eigenvalues (not shown here) were all negative, consistent with being near the observable maximum at $P_{|1\rangle \rightarrow |8\rangle} = 0.99$. Figure 2 displays the trace of the Hessian, $\int_0^T \mathcal{H}(t, t) dt$, for level set trajectories taken in both the fluence maximizing and fluence minimizing directions. Since these trajectories originate with the same control field $E(s=0, t)$, Fig. 2 is naturally continuous. There is a cusp at $s=0$ arising from a slope discontinuity due to the differences between the constants c_{\pm} employed in $f_{\pm}(s, t)$, Eq. (18). As the field grows in amplitude (i.e., the fluence maximizing trajectory), the trace of the Hessian is not preserved. The variation in the trace reflects the existence of different degrees of robustness of the observable $\langle \mathcal{O}(s) \rangle$ to noise in the control field $E(s, t)$, despite the fact that $\langle \mathcal{O}(s) \rangle = \langle \mathcal{O}(s=0) \rangle$ is a dynamical constant on the level set. Conversely, along the field minimizing trajectory, the trace of the Hessian varies slightly and then approaches a limiting value. This less dramatic behavior is consistent with Fig. 1(a), where $E_-(s, t)$ quickly approaches a limiting pulse shape as s increases.

These calculations and many others (not shown here) clearly show the ability to move freely over control landscape level sets at high target observable yields. In doing so, continuous families of fields may be identified of rich, evol-

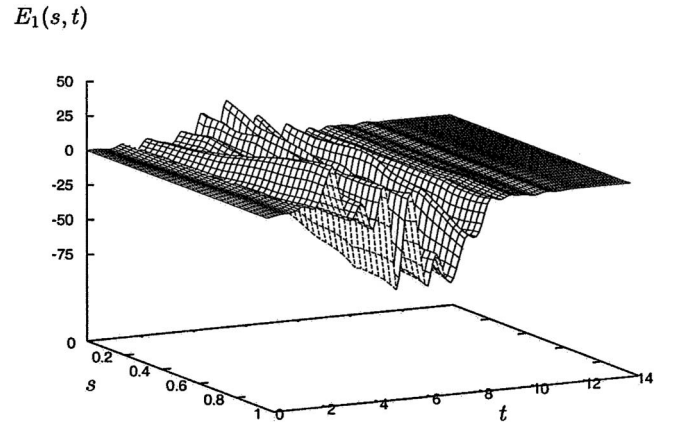


FIG. 3. The control fields along the level set described by $f_1(s, t)$ are displayed. The control field continually changes with s ; at $s=1$, it has a substantially different envelope structure than the field at $s=0$, due to the influence of $f_1(s, t)$. Yet fields along the entire s interval render the same value of the target observable population of 0.47.

ing structure where each field in the family preserves the high yield of the target observable, yet has its own associated control mechanism and other dynamical properties.

B. Level sets for low control yield

To explore the properties of suboptimal level sets (i.e., $P_{|i\rangle \rightarrow |f\rangle}$ significantly less than unity) in the control landscape, again consider the same quantum system [29] for the control goal $|1\rangle \rightarrow |8\rangle$. In this case, the initial control field $E(s=0, t)$ produces a population transfer of 0.47 into state $|8\rangle$. This example in conjunction with the one above aims to illustrate that the level-set explorations can be done at any objective value and further reveals variations of the controlled dynamics across the level set. The function $f(s, t)$ will be chosen distinct from the case in Sec. III A to showcase the flexibility inherent in the level-set trajectory method. In particular, we choose $f_1(s, t) = 25(s+1)[S(t+3) - S(t-1)]$, where $S(t)$ is the weight function used in the previous example. Figure 3 displays the control fields $E_1(s, t)$, exhibiting vastly different structure over the s interval, guided by the function $f_1(s, t)$. To highlight the dramatic differences in control mechanism encountered along the level set, Fig. 4 displays the population of selected states at $s=0$ [Fig. 4(a)], $s=0.5$ [Fig. 4(b)], and $s=1$ [Fig. 4(c)] (the population of all eight states is not shown for clarity). The dynamics reacts to the differences in control field structure as s increases, including highly oscillatory behavior at $s=1$. These populations demonstrate that significantly different control mechanisms operate at each s value; however, the population in state $|8\rangle$ at time T remains fixed to within arbitrary precision despite the presence of intermediate dynamics of varying complexity. This calculation indicates that the level-set trajectories in the quantum control landscape can traverse a continuous variety of control fields, showing widely varying structure and producing distinct dynamics, except for preservation of the same final yield at $t=T$. Despite the diverse behavior of $E(s, t)$ shown

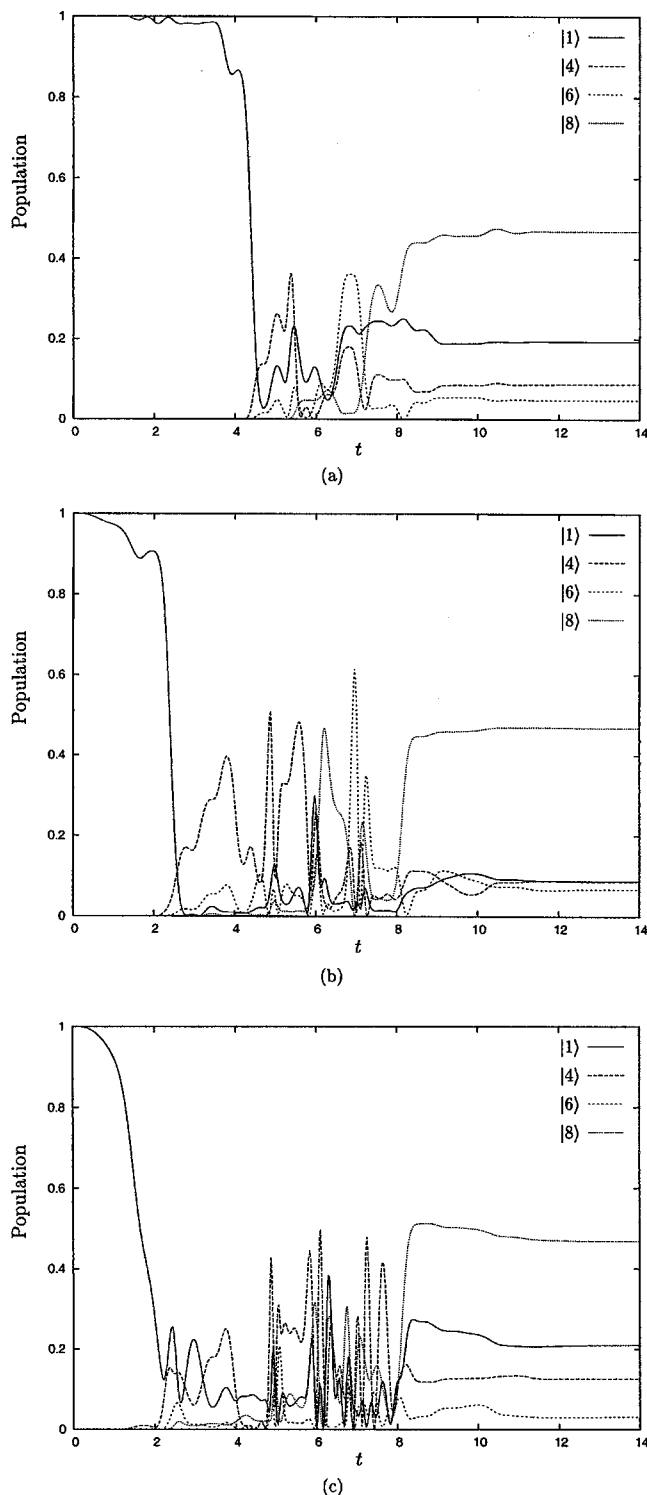


FIG. 4. The intermediate-time dynamics are displayed for states $|1\rangle$, $|4\rangle$, $|6\rangle$, and $|8\rangle$ at (a) $s=0$, (b) $s=0.5$, and (c) $s=1$. The populations of the states not pictured show similar oscillatory behavior and are omitted to make the figures more clear. Importantly, despite the differences in the controlled dynamics, the population of state $|8\rangle$ at $t=T$ remains fixed at 0.47 for all s . The dynamics appear to gain complexity with s , indicating that distinct control mechanisms must operate at each s value that leave the final population of state $|8\rangle$ unchanged.

across a level set, even a slight arbitrary disturbance $\delta E(s, t)$, such that $E(s, t) \rightarrow E(s, t) + \delta E(s, t)$, will generally alter the dynamics to produce $\langle O(s) \rangle \neq \langle O(s=0) \rangle$ at time T , corresponding to movement off the level set. The trace of the Hessian was also calculated along the level set trajectory in this example (not shown here), and more extensive variations were found upon scanning s than for the illustration in Fig. 2.

IV. CONCLUSION

Quantum control landscapes are an inherent feature of controlled quantum dynamics [20]. However, the nature of the landscapes and their structures for general observables is only beginning to be understood. This paper takes a step in that direction by presenting a computationally practical technique for traversing arbitrary paths along the level sets in a landscape. The existence of a continuous function $f(s, t)$ of arbitrary shape is critical in this regard, as a choice of $f(s, t)$ determines a specific trajectory through the landscape level set. The level-set formulation in Sec. II is general and may be applied to considering the control of arbitrary quantum systems. The illustrations in the paper are only glimpses of particular landscape level sets in simple systems; however, the general findings are revealing and should carry over to the control of other quantum systems. It is evident that a continuous family of fields can be found which are capable of producing the same control objective value [27]. Perhaps the most striking finding is the vastly different nature of the control fields that can inhabit a level set and the concomitant unique, rich dynamics that each control field produces while still producing the same target value at $t=T$.

The examples with $E_+(s, t)$ and $E_-(s, t)$ in Sec. III A reveal a landscape geometry which is likely operative in many circumstances. In particular, a level set will always have a forbidden domain around $E(s, t)=0$, as some minimal amount of quantum-mechanical action is needed to effect the desired control process. At the other extreme, the level sets can nominally be unbounded in extent (in terms of field metric $D_s[E]$), with fields of increasing strength and structure being important factors that can produce complex dynamical processes. Practical limits may exist in many cases, since new undesired physics may open up in moving to the outer boundaries of a level set, eventually forbidding satisfaction of the level set value (e.g., dissociating a molecule when the level set goal was vibrational excitation). Nevertheless, the level sets are expected to still be unbounded with possibly some inaccessible domains to avoid the occurrence of certain dynamical processes. In the laboratory, the controls are inevitably limited in their freedom due to a variety of factors (e.g., pulse energy, bandwidth, etc.), and these constraints can impose artificial structure on the landscape and level sets.

The distinct dynamics produced by different members of the level set also shows that the fields are not just differing in some trivial fashion (e.g., by introducing frequency components that do not address the system transitions, even though such level-set members must exist as well). Each level-set field can manipulate the dynamics in its own special way, likely also including dynamic power shifting of the system's

energy levels in the process. The diversity of level-set dynamical behavior also implies an associated richness in the mechanisms of controlled quantum-dynamics phenomena. A well-posed quantum control problem can have a variety of successful control mechanisms. Although some mechanisms perhaps may be deemed more desirable by being simpler than others, that assessment is a matter of judgment and not a fundamental issue. As shown in the illustration of Sec. III A, it may at times be true that controls of minimal fluence tend to produce simpler mechanisms.

In addition to the control mechanisms morphing over the level set, all other dynamical properties (except $\langle \mathcal{O} \rangle$ defining the level set) should vary. The particular property of observable robustness to control variations (i.e., noise) was illustrated in Sec. III A. The variation of such properties over the level set opens up the prospect of seeking sublevel sets that either preserve some other dynamical property (while still leaving the target observable value constant) or, alternatively, extremize its value. One possible means for identifying sublevel sets that satisfy the former criterion would be to introduce additional projectors into Eq. (13) with the aim of projecting off the components of any continuous function $f(s, t)$ that change the dynamical property desired to be conserved.

The common experience of finding one particular optimal field in laboratory control experiments or in simulations does not reveal the full picture of the controlled dynamics. The ability to transform one successful control into another, and therefore one control mechanism into another, should be considered when seeking to establish the “mechanism” in any particular quantum control problem. In this regard, it would be most valuable to directly search for the control level sets in the laboratory, and some observables may be more amenable to such an analysis than others (i.e., experiments confined to the weak-field regime may provide fewer options for level-set exploration while operating at too high intensities could introduce undesired physical processes). Recent experimental control studies [17,28,29], performed for other reasons, when interpreted properly already show the existence of control level sets. More focused efforts at revealing the level sets would be most desirable, and in this regard the coefficients in Eq. (5) could be extracted from laboratory data for level-set exploration followed by a step $E(s, t) \rightarrow E(s + \Delta s, t)$ taken with a choice for $f(s, t)$. Directly assigning the laboratory search algorithms to explore a level set would be valuable. Such experimental landscape studies, as well as additional theoretical analysis, should better reveal the full nature of controlled quantum-dynamics phenomena.

ACKNOWLEDGMENT

The authors acknowledge support from the National Science Foundation and ARO-MURI grants. In addition, con-

versations with M. Hsieh regarding the topology of the quantum control landscapes have provided valuable insights.

APPENDIX

This appendix derives the expression for $a_0(s, t)$ in Eq. (6). Starting from the Schrödinger equation (1), consider a variation in the wave function $\delta|\psi(t)\rangle$ with respect to a corresponding variation in the control field $\delta E(s, t')$. The relationship may be expressed as

$$\begin{aligned} i\hbar \frac{\partial}{\partial t} \left(\frac{\delta|\psi(t)\rangle}{\delta E(s, t')} \right) &= \mathcal{H}_0 \frac{\delta|\psi(t)\rangle}{\delta E(s, t')} - \mu \left[\frac{\delta E(s, t)}{\delta E(s, t')} |\psi(t)\rangle + E(s, t) \frac{\delta|\psi(t)\rangle}{\delta E(s, t')} \right] \\ &= [\mathcal{H}_0 - \mu E(s, t)] \frac{\delta|\psi(t)\rangle}{\delta E(s, t')} - \mu \delta(t - t') |\psi(t)\rangle. \end{aligned} \quad (\text{A1})$$

Equation (A1) is an inhomogeneous equation for the functional derivative $\frac{\delta|\psi(t)\rangle}{\delta E(s, t')}$, with zero initial condition at $t=0$. The solution to Eq. (A1) is

$$\begin{aligned} i\hbar \frac{\delta|\psi(T)\rangle}{\delta E(s, t')} &= - \int_0^T U(T, t') \mu \delta(t' - t'') |\psi(t'')\rangle dt'' \\ &= - U(T, t') \mu |\psi(t')\rangle \\ &= - U(T, 0) U^\dagger(t', 0) \mu U(t', 0) |\psi_0\rangle. \end{aligned} \quad (\text{A2})$$

Using this relation, the coefficient $a_0(s, t)$ may be determined,

$$\begin{aligned} a_0(s, t) &\equiv \frac{\delta \langle \mathcal{O} \rangle}{\delta E(s, t)} = \frac{\delta}{\delta E(s, t)} [\langle \psi(T) | \mathcal{O} | \psi(T) \rangle] \\ &= \langle \psi(T) | \mathcal{O} \left| \frac{\delta \psi(T)}{\delta E(s, t)} \right\rangle + \text{c.c.} \\ &= - \frac{1}{i\hbar} \langle \psi_0 | U^\dagger(T, 0) \mathcal{O} U(T, 0) U^\dagger(t, 0) \mu U(t, 0) | \psi_0 \rangle \\ &\quad + \text{c.c.} \\ &= - \frac{1}{i\hbar} \langle \psi_0 | [U^\dagger(T, 0) \mathcal{O} U(T, 0), U^\dagger(t, 0) \mu U(t, 0)] | \psi_0 \rangle, \end{aligned} \quad (\text{A3})$$

which is Eq. (6).

-
- [1] H. Rabitz, R. de Vivie-Riedle, M. Motzkus, and K. Kompa, *Science* **288**, 824 (2000).
 [2] S. A. Rice and M. Zhao, *Quantum Control of Molecular Dynamics* (Wiley-Interscience, New York, 2000).
 [3] S. Shi and H. Rabitz, *J. Chem. Phys.* **92**, 364 (1990).

- [4] J. P. Palao and R. Kosloff, *Phys. Rev. A* **68**, 062308 (2003).
 [5] H. Rabitz and W. Zhu, *Acc. Chem. Res.* **33**, 572 (2000).
 [6] R. Kosloff, S. A. Rice, P. Gaspard, S. Tersigni, and D. J. Tannor, *Chem. Phys.* **139**, 201 (1989).
 [7] A. P. Peirce, M. A. Dahleh, and H. Rabitz, *Phys. Rev. A* **37**,

- 4950 (1988).
- [8] R. de Vivie-Riedle, K. Sundermann, and M. Motzkus, *Faraday Discuss.* **113**, 303 (1999).
- [9] J. Geremia, W. Zhu, and H. Rabitz, *J. Chem. Phys.* **113**, 10841 (2000).
- [10] W. S. Zhu and H. Rabitz, *J. Chem. Phys.* **109**, 385 (1998).
- [11] G. Balint-Kurti, F. Manby, Q. Ren, M. Artamonov, T.-S. Ho, and H. Rabitz, *J. Chem. Phys.* **122**, 084110 (2005).
- [12] R. S. Judson and H. Rabitz, *Phys. Rev. Lett.* **68**, 1500 (1992).
- [13] C. J. Bardeen, V. V. Yakovlev, K. R. Wilson, S. D. Carpenter, P. M. Weber, and W. S. Warren, *Chem. Phys. Lett.* **280**, 151 (1997).
- [14] M. Renard, E. Hertz, B. Lavorel, and O. Faucher, *Phys. Rev. A* **69**, 043401 (2004).
- [15] T. Brixner, G. Krampert, T. Pfeifer, R. Selle, G. Gerber, M. Wollenhaupt, O. Graefe, C. Horn, D. Liese, and T. Baumert, *Phys. Rev. Lett.* **92**, 208301 (2004).
- [16] A. Lindinger, M. Plewicky, S. M. Weber, C. Lupulescu, and L. Woste, *Opt. Appl.* **34**, 341 (2004).
- [17] D. Cardoza, C. Trallero-Herrero, F. Langhojer, H. Rabitz, and T. Weinacht, *J. Chem. Phys.* **122**, 124306 (2005).
- [18] G. Vogt, G. Krampert, P. Niklaus, P. Nuernberger, and G. Gerber, *Phys. Rev. Lett.* **94**, 068305 (2005).
- [19] A. Lindinger, S. M. Weber, C. Lupulescu, F. Vetter, M. Plewicky, A. Merli, L. Woste, A. F. Bartelt, and H. Rabitz, *Phys. Rev. A* **71**, 013419 (2005).
- [20] H. A. Rabitz, M. H. Hsieh, and C. M. Rosenthal, *Science* **303**, 1998 (2004).
- [21] M. Demiralp and H. Rabitz, *Phys. Rev. A* **47**, 831 (1993).
- [22] H. Shen, J.-P. Dussault, and A. D. Bandrauk, *Chem. Phys. Lett.* **221**, 498 (1994).
- [23] V. S. Malinovsky and D. J. Tannor, *Phys. Rev. A* **56**, 4929 (1997).
- [24] A. Rothman, T.-S. Ho, and H. Rabitz, *Phys. Rev. A* **72**, 023416 (2005).
- [25] The function $f(s,t)$ could be chosen as discontinuous or with other unusual features, but these would in turn be reflected in the control $E(s,t)$. Thus, on physical grounds $f(s,t)$ is restricted to continuous functions.
- [26] The matrix \mathcal{H}_0 is diagonal with elements 1.0, 5.0, 8.5, 11.0, 13.0, 14.7, 16.1, and 17.3. The nonzero elements of μ were 0.15 for adjacent levels, 0.08 for next-nearest-neighbor interactions, and 0.01 for transitions through two intermediate states.
- [27] The work presented here does not strictly exclude the possibility of other disjoint field sets existing with the same level set value for the target observable.
- [28] A. F. Bartelt, M. Roth, M. Mehendale, and H. Rabitz, *Phys. Rev. A* **71**, 063806 (2005).
- [29] E. Wells, K. Betsch, C. W. S. Conover, M. J. DeWitt, D. Pinkham, and R. R. Jones, *Phys. Rev. A* **72**, 063406 (2005).